ISSN 1063-7397, Russian Microelectronics, 2019, Vol. 48, No. 8, pp. 531–544. © Pleiades Publishing, Ltd., 2019.
Russian Text © The Author(s), 2017, published in Izvestiya Vysshikh Uchebnykh Zavedenii, Materialy Elektronnoi Tekhniki, 2017, Vol. 20, No. 3, pp. 183–196.

Peculiarities of the Crystal Structure and Texture of Isotropic and Anisotropic Polycrystalline Hexagonal Ferrites $BaFe_{12}O_{19}$ Synthesized by Radiation-Thermal Sintering

I. M. Isaev[a], S. V. Shcherbakov[b], V. G. Kostishin[a, *], A. G. Nalogin[b], V. V. Mokljak[c], B. K. Ostafijchuk[d], A. A. Alekseev[a, b], V. V. Korovushkin[a], E. A. Belokon'[a, b], M. V. Kalinyuk[d], M. A. Mihaylenko[e], M. V. Korobeynikov[e], A. A. Bryazgin[e], and D. V. Salogub[a]

[a]*National University of Science and Technology MISIS, Moscow, 119049 Russia*
[b]*AO NPP Istok im. Shokina, Fryazino, Moscow oblast, 141190 Russia*
[c]*Kurdyumov Institute for Metal Physics, National Academy of Sciences, Kiev, 03680 Ukraine*
[d]*Stefanyk Precarpathian National University, Ivano-Frankivs'k, 76025 Ukraine*
[e]*Budker Institute of Nuclear Physics, Siberian Branch, Russian Academy of Sciences, Novosibirsk, 630090 Russia*
**e-mail: drvgkostishyn@mail.ru*

Received May 10, 2018

Abstract—In this work the crystal structure and texture of isotropic and anisotropic polycrystalline hexagonal ferrites $BaFe_{12}O_{19}$ obtained by the method of radiation-thermal sintering (RTS) is studied using X-ray diffraction and X-ray phase analysis. Crude blanks of both isotropic and anisotropic hexaferrites are obtained by the standard method of ceramic technology from the same raw material (Fe_2O_3 and $BaCO_3$ of the analytical grade brand) and on the same equipment with the only difference being that the anisotropic blanks were pressed in the magnetic field $H = 10$ kOe. For sintering raw billets, a linear electron accelerator ILU-6 (electron energy $E_e = 2.5$ MeV) is used (Budker Institute of Nuclear Physics, Siberian Branch, Russian Academy of Sciences). The samples are sintered in air for one hour at 1200, 1250, 1300, and 1350°C. It is shown for the first time that high-quality single-phase isotropic and anisotropic hexaferrites $BaFe_{12}O_{19}$ can be obtained from raw blanks of a ferritized charge using the RTS technology. The properties of the crystal structure and texture of the obtained objects of the research are described. It is established for the first time that the dependence of the pref.orient.o1 predominant orientation of the crystal texture parameter on the degree of the magnetic texture f in polycrystalline hexagonal barium ferrites of type M is described by the expression pref.orient.o1 = $-0.005f + 0.6886$.

Keywords: hexagonal polycrystalline ferrite $BaFe_{12}O_{19}$, isotropic hexaferrite, anisotropic hexaferrite, crystal structure, crystal texture, magnetic texture, texture degree, parameter pref.orient.o1, ferritized charge, compaction in a magnetic field

DOI: 10.1134/S1063739719080079

INTRODUCTION

The crystal structure of $BaFe_{12}O_{19}$ hexagonal ferrites has a magnetoplumbite $PbFe_{12}O_{19}$ lattice. This structure was studied first by Adelsköld in 1938 [1]. Complex substituted polycrystalline barium hexaferrites are used in making circulators, switches, resonators, filters, and phase shifters operating in the frequency range of 1 to 110 GHz due to their high values of resistivity and permeability for the SHF electromagnetic field [2–11]. The anisotropic (texturized) complex substituted polycrystalline hexagonal ferrites are especially promising among this class of materials. They are magnetically uniaxial and possess high magnetic anisotropy fields [4, 8–11]. Use of these materials in resonance-type ferrite SHF devices allows decreasing the intensity of the external field and, hence, the size and weight of the whole magnetic system [11].

Ceramic technology is today the most often used industrial method of obtaining isotropic and anisotropic polycrystalline hexagonal ferrites [9, 10, 12–17]. The main disadvantages of this technology are high energy consumption, long duration of the process, and low success yield. Radiation-thermal sintering (RTS) may become an alternative to the classical ceramic technology of the synthesis of barium hexaferrites. This is a technology based on sintering by flows of fast electrons, which has shown its unique possibilities in the synthesis of polycrystalline ferrites with different compositions [18–41]. The advantages of RTS are its speed and quick response of heating, absence of contact between the heated body and the heater, uniform

Table 1. Information about batches of crude samples of the synthesized and studied objects of investigation

Batch name	Chemical composition	Number of samples	Comment
BH-12A	$BaFe_{12}O_{19}$	5	Anisotropic
BH-12I	$BaFe_{12}O_{19}$	5	Isotropic

character of heating over the whole volume, and, above all, the energy efficiency and speed of the technological process [18–41]. The radiation-thermal method has shown its unique possibilities in synthesizing and sintering some complex oxides and portland cement clinkers, as well as uncovering and enriching mineral raw materials. Systematic studies on the radiation-thermal synthesis of lithium ferrites were carried out at Tomsk Polytechnic University by the group led by Prof. A.P. Surzhikov [18–29]; and the RTS of Mn–Zn-, Mg–Zn and Ni–Zn-ferrites was investigated at the Department of Electronics Materials Technology (National University of Science and Technology MISIS) by the group led by Prof. V.G. Kostishin [30–37, 40]. Detailed studies of the radiation-thermal activation of diffusion are presented in the scientific publications of researchers from Tomsk. The Tomsk scientific school (A.P. Surzhikov, S.A. Gyngazov, A.M. Pritulov, Yu.M. Annenkov and others) is a word leader in investigating the RTS of ferrites. Note that there are a few publications devoted to investigating the influence of RTS on the properties of type W hexaferrites only, and these works do not contain complex studies [42–44]. Apart from publications [38, 39, 41] by the authors of this work, we have not found any published scientific papers that have presented the results on the RTS of isotropic and anisotropic polycrystalline hexagonal type M ferrites.

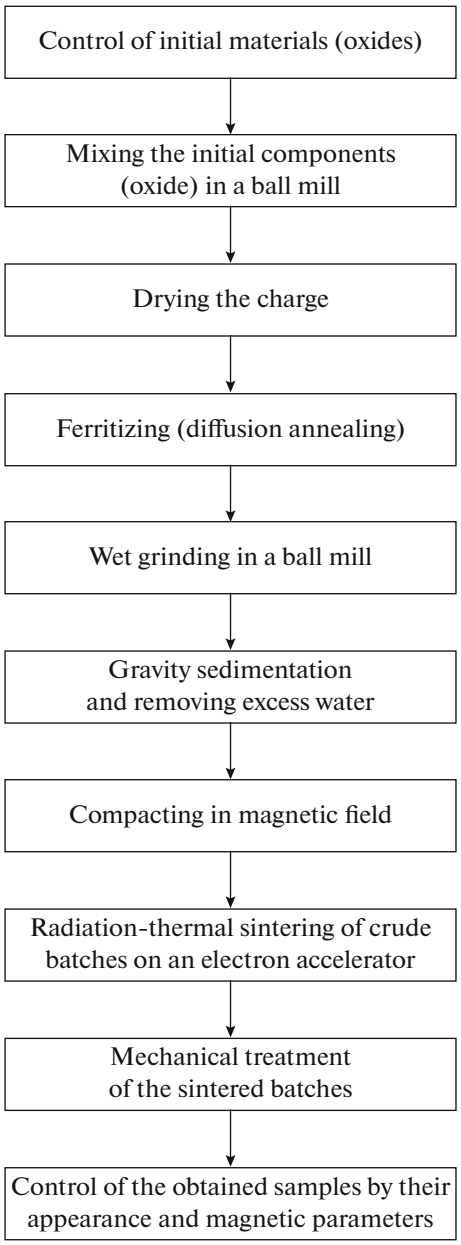

Fig. 1. Technological scheme for obtaining anisotropic hexagonal polycrystalline ferrites by the RTS method.

The aim of this work is to study the possibility of using the RTS technology to obtain high-quality isotropic and anisotropic hexaferrite $BaFe_{12}O_{19}$ for making permanent magnets and substrates of microstrip SHF electronic devices.

1. EXPERIMENTAL

1.1. Objects of Study and Their Preparation

Isotropic and anisotropic polycrystalline hexagonal barium ferrites prepared by the RTS method were the objects chosen for synthesis and investigation. Crude blanks of polycrystalline hexaferrite $BaFe_{12}O_{19}$ were made following the standard ceramic technology. Information about every batch of the crude samples is given in Table 1.

Analytical-pure grade reagents were used as the raw materials: iron oxide Fe_2O_3 (standard TU 6-09-5346-87) and barium carbonate $BaCO_3$ (GOST (State Standard) 4158-80). Barium carbonate is decomposed into barium oxide and carbon dioxide (CO_2) at temperatures above 1000°C. The technological scheme used for obtaining anisotropic hexaferrites by RTS is shown in Fig. 1.

The initial components were mixed for 24 h in a ball mill with the following ratios: balls : charge : water = 2 : 1 : 1. After mixing the charge was put in a dish made

of stainless steel and placed in a drying chamber, where it was held at 130°C until the water was totally removed. After drying the charge was ground through a sieve and poured out into a nickel dish. Then the charge was put into a silite electric stove and ferritized. The ferritizing annealing temperature was 1150°C for the batches of strontium hexaferrite (SH) and 1250°C for barium hexaferrite (BH). The isothermal exposition time was 5 h. After completion of the ferritizing process, the charge was wet ground in the ball mill with the same proportion of the balls, charge, and water for 96 h. The suspension obtained after wet milling was poured into a vessel and was allowed to settle under normal conditions for 3 days or more. Then the excess water was removed and the dense suspension obtained was compacted. The moisture content of the suspension before the compaction procedure was about 30–35%.

Hexaferrite samples were compacted in a mould with a brass matrix and punches made from soft-magnetic steel. The mould allows applying a magnetic field in the gap between the punches where the suspension to be texturized is placed. The bottom punch is covered by a felt filter and has holes to remove the water through the filter. In addition, the punches are furnished with filters made from a cotton sheeting to prevent the samples from sticking.

The magnetic field was generated by an electromagnet made of two coils fastened on a frame. The frame works also as a magnetic circuit. The ram of the press with a tip attached to it goes through the upper coil. The tip shape is chosen to concentrate the magnetic field. Inside the bottom coil the base of the mould is placed with an outlet for water, which ends with a pipe connection, and the pipe connects it to a fore vacuum pump through a trap.

The anisotropic blanks were compacted with the magnetic field applied along the pressing direction. The excess water was removed from the mould with the aid of the fore vacuum pump through the channels in the bottom punch and filtering elements for 5 min with the magnetic field turned on. The optimal compacting pressure was used, which allows obtaining dense samples without cracks and delamination. The field intensity during the compaction process was 10 kOe.

The isotropic blanks of barium hexaferrite were compacted by following the same procedure as for the anisotropic ones (see Fig. 1), using the same instruments and operation regimes, with the only difference that no field was applied during the compaction process.

The residual moisture content of the compacted blanks was nearly 10%.

The compacted blanks were dried under ambient conditions for at least 2 days and then were subject to sintering.

The RTS of the crude blanks was carried out using fast electrons on a 2.5-MeV ILU-6 linear accelerator designed for radiation technologies at the Budker Institute of Nuclear Physics (Siberian Branch, Russian Academy of Sciences). A special cell for radiation-thermal sintering was designed and built for use in this research study [45].

Five anisotropic and five isotropic crude blanks of hexaferrite $BaFe_{12}O_{19}$ were created by the RTS method at temperatures of 1200, 1250, 1300, and 1350°C. The temperature growth rate in the sintering process was 50°C/min; the duration of the process was varied from 10 to 120 min. The RTS temperatures, heating rate, and duration were chosen based on the published data on sintering barium hexaferrites following the traditional ceramic technology [2–4, 9, 10, 12–17] and also using the experience on sintering the ferrite ceramics gained by the authors' team.

1.2. X-ray Phase and Structural Analysis of the Objects of Study

The X-ray phase and structural analysis of the objects was carried out on a DRON-8 diffractometer (AO NPP Burevestnik, St. Petersburg, Russia).

CoK_{α_1} radiation was used in the analysis. The wavelength was $\lambda = 0.178897$ nm. The Bragg–Brentano focusing geometry with two Soller slits was used. The measurements were performed at room temperature.

The Powder Cell 2/4 software was used for data processing. The most correct interpretation of the X-ray diffraction patterns was achieved when the March/Dollase model of the presence of a predominant orientation was chosen [46], that is, when the presence of a crystalline texture in the studied objects was assumed. The parameter pref.orient.o1 [46] is the main characteristic of the texture in this case: it points to the texture type and characterizes the relative influence of the texture on the intensity of the corresponding reflexes. The following variants are possible:

pref.orient.o1 > 1, needles;

pref.orient.o1 < 1, plates;

pref.orient.o1 = 1, total disorientation and absence of texture.

To determine the degree of the magnetic texture, the sample was fastened on a holder by the plane perpendicular to the hexagonal axis, which should coincide with the texture's direction, and then the intensities of the basic and the reference lines were compared.

Lines ⟨008⟩ and ⟨107⟩ are most intensive and hence most convenient in the case of barium hexaferrites. Similar measurements were made for the isotropic sample with the same composition. The degree of the magnetic texture was evaluated as

$$f = (P - P_0)/(1 - P_0) \times 100\%, \quad (1)$$

where $P_0 = I^0_{008}/(I^0_{008} + I^0_{107})$; $P = I_{008}/(I_{008} + I_{107})$;

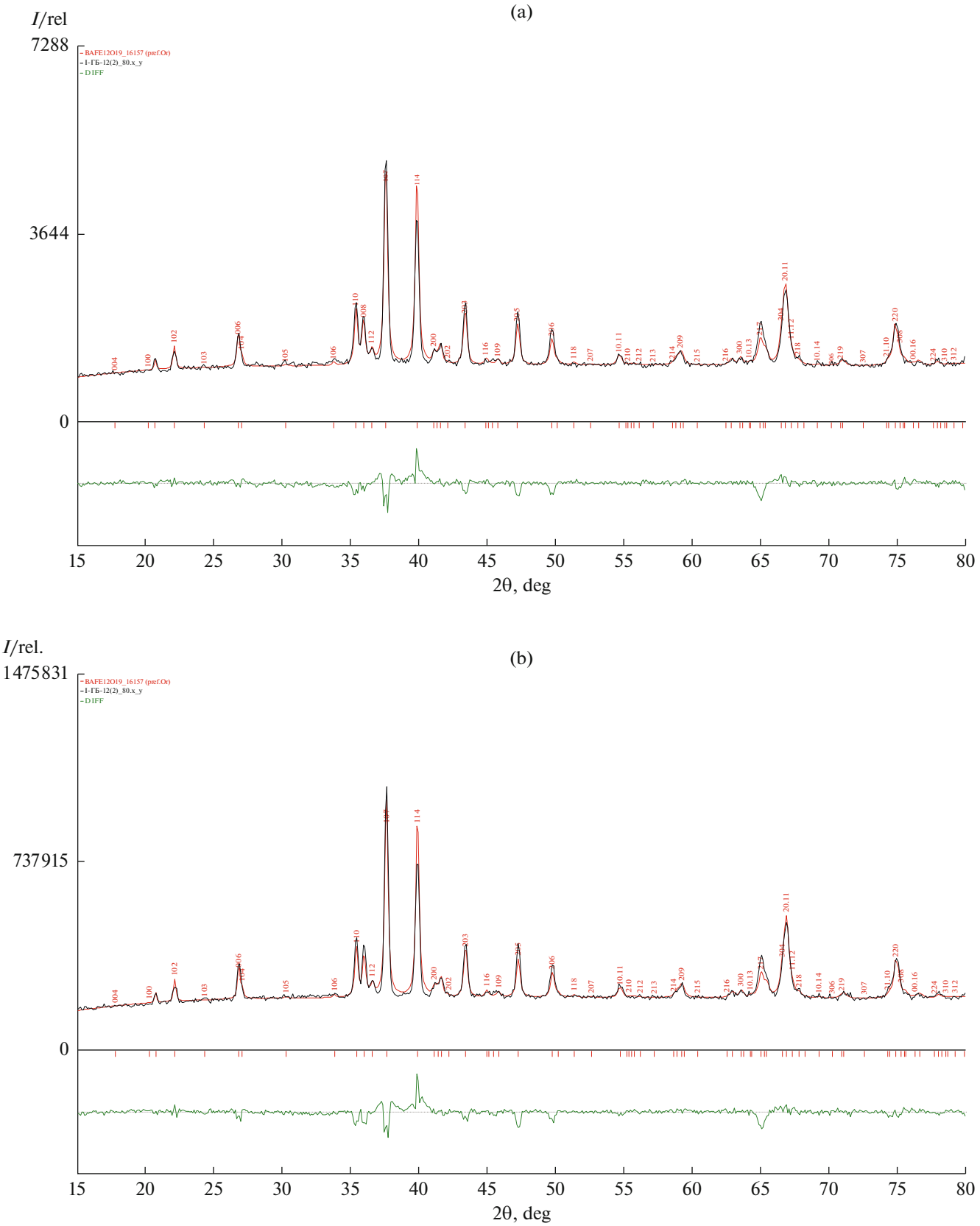

Fig. 2. Typical X-ray diffraction pattern of isotropic hexaferrite $BaFe_{12}O_{19}$ (batch BH-12I) obtained by RTS at (a) 1200 and (b) 1250°C. 2θ values cover the range from 15° to 80°. Black line shows experimental data; red line, model; green line, difference spectrum.

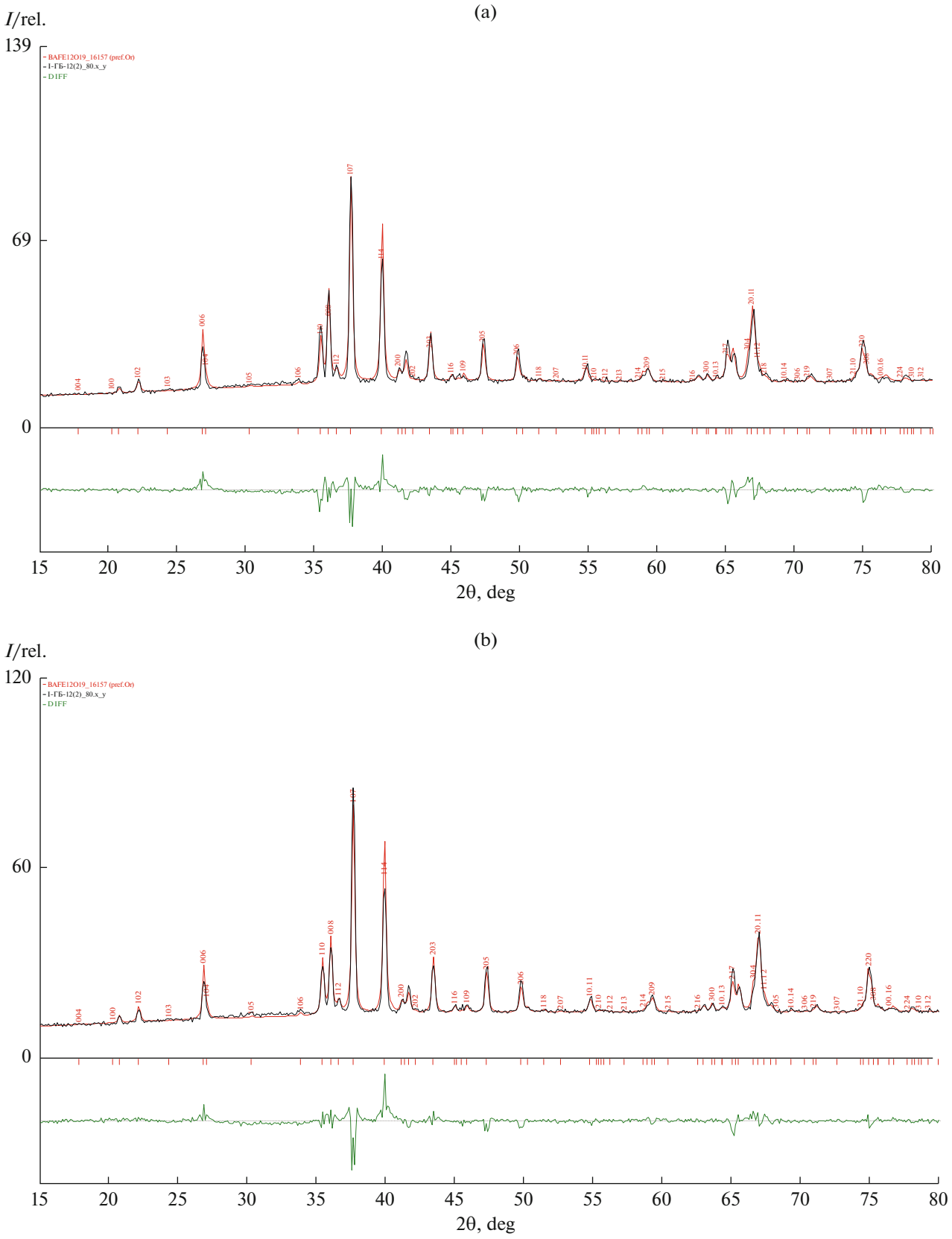

Fig. 3. Typical X-ray diffraction pattern of isotropic hexaferrite $BaFe_{12}O_{19}$ (batch BH-12I) obtained by RTS at (a) 1300 and (b) 1350°C. 2θ values cover the range from 15° to 80°. Black line shows experimental data; red line, model; green line, difference spectrum.

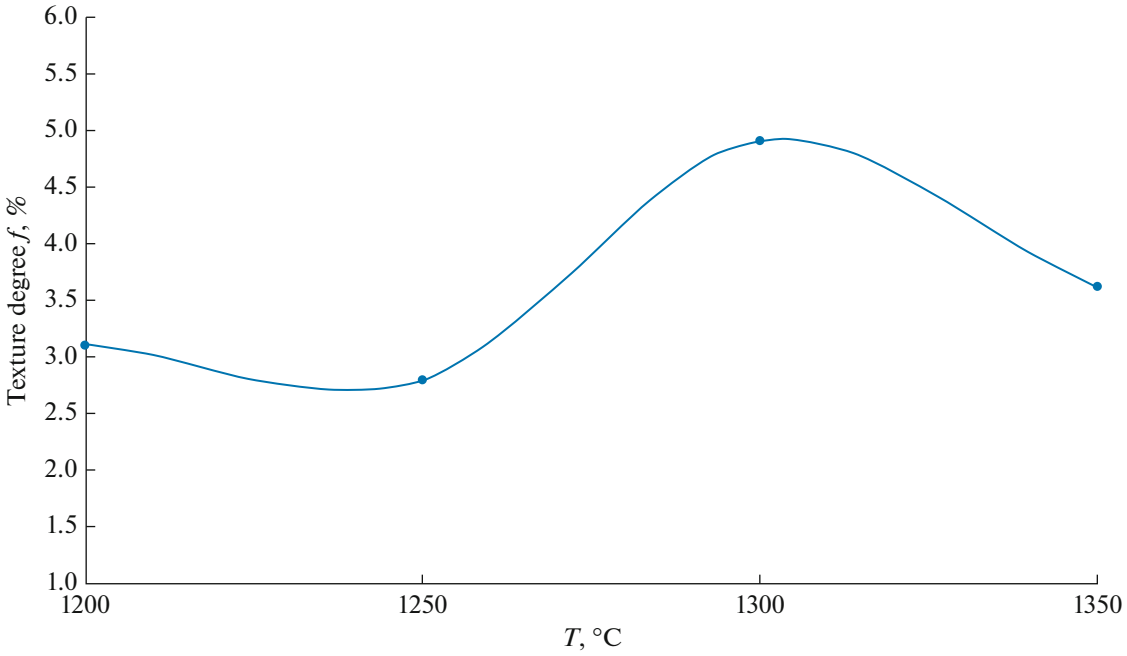

Fig. 4. Dependence of the degree of magnetic texture on the RTS temperature for the samples of isotropic hexaferrite $BaFe_{12}O_{19}$ (batch BH-12I).

the values of I^0_{008}, I^0_{107}, $I_{008,}$ and I_{107} are the intensities of the basic and the reference lines for the non-textured and textured samples, respectively.

2. RESULTS AND DISCUSSION

2.1. Isotropic Hexaferrite $BaFe_{12}O_{19}$

Figures 2 and 3 present the typical X-ray diffraction patterns of the samples of isotropic hexaferrite $BaFe_{12}O_{19}$ (batch BH-12I) prepared by the RTS process during 1 h at the sintering temperatures of 1200 (Fig. 2a), 1250 (Fig. 2b), 1300 (Fig. 3a), and 1350°C (Fig. 3b).

All the samples consist of a single phase, and their crystal structure corresponds to that of barium hexaferrite $BaFe_{12}O_{19}$ (ICSD #16157) [47]. All the samples are characterized by a prominent plate-type texture with the parameter pref.orient.o1 in the range of 0.66 to 0.74. As the sintering temperature increases, the shear plane of the plates (actually, their surface) changes from (107) when sintered at 1200 and 1250°C to (001) when prepared at 1300 and 1350°C. The change is clearly seen from the intensity ratio of the reflexes (107) and (008) on the X-ray diffraction patterns of the corresponding samples.

The X-ray diffraction data and calculations using Eq. (1) revealed that the degree of the magnetic texture of isotropic hexaferrites after RTS at T = 1200–1250°C is about 3%, it increases further to 4.9% at T = 1300°C, and at the sintering temperature of T = 1350°C the degree of the texture decreases to 3.6% (Fig. 4).

The presence of slight magnetic texturizing in isotropic hexaferrites is a well-known fact [48]. This texture is due to the lamellar shape of the hexaferrite particles which are formed in the ferritizing process. The particles of hexaferrite are oriented with their planes normal to the pressing axis during compaction of the crude blank of isotropic hexaferrite even without a magnetic field. As a result, the magnetic texture arises and becomes more prominent at an increasing sintering temperature [48].

The temperature dependences of the lattice parameters (a and c) and of the size of the coherence scattering region (CSR) of isotropic hexaferrites $BaFe_{12}O_{19}$ (batch BH-12I) are shown in Fig. 5. Evidently, the lattice parameter a increases first (at $T > 1250$°C), and it begins to decrease above 1300°C. Parameter c decreases significantly as the RTS temperature grows. The CSR size shows a somewhat less prominent tendency to decrease as the temperature grows.

2.1. Anisotropic Hexaferrite $BaFe_{12}O_{19}$

Figures 6 and 7 present the X-ray diffraction patterns of the samples of anisotropic hexaferrite $BaFe_{12}O_{19}$ (batch BH-12A) prepared in the RTS process at the sintering temperatures of 1200, 1250, 1300, and 1350°C.

All samples are monophasic, and their crystal structure corresponds to that of barium hexaferrite

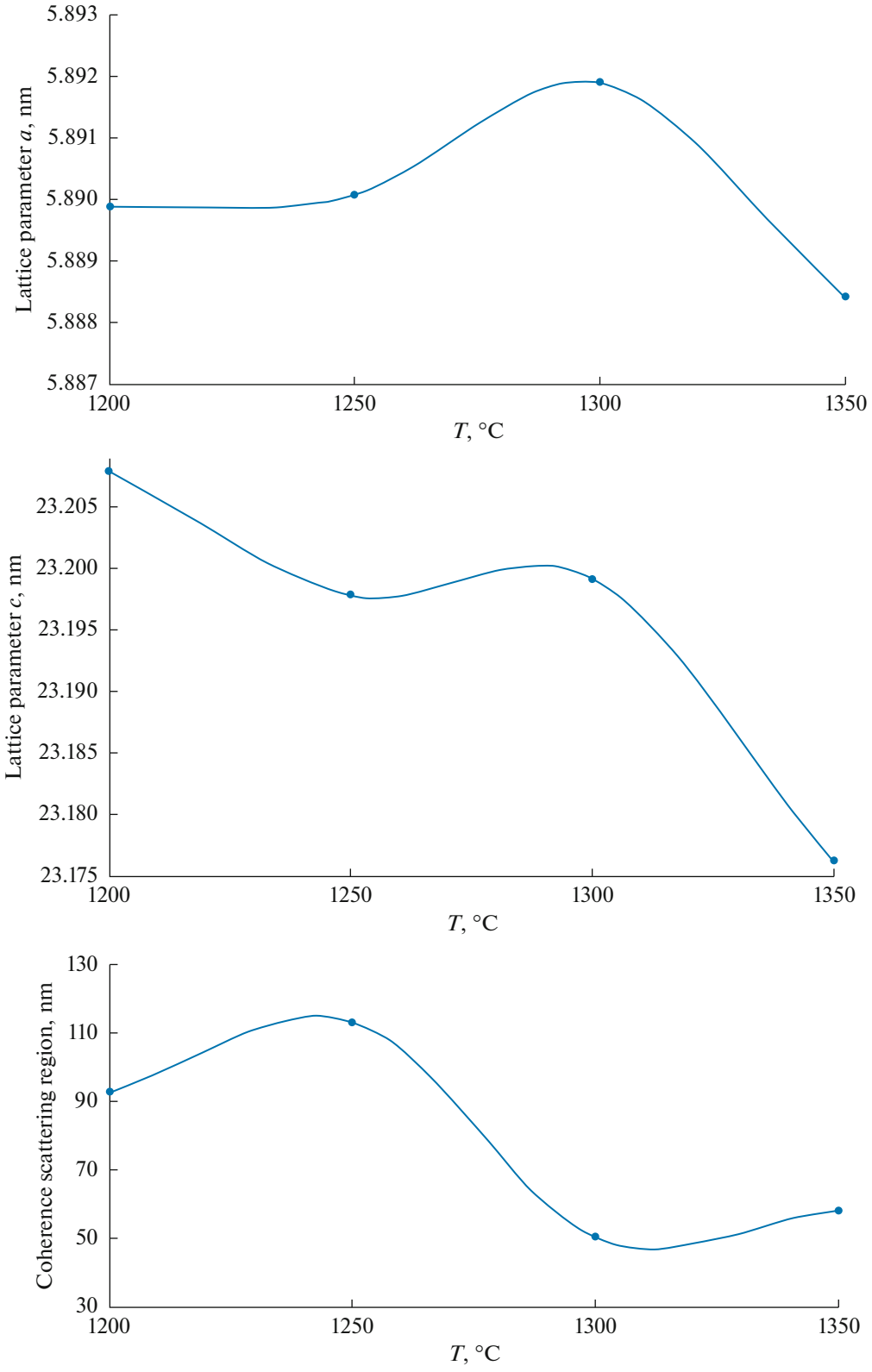

Fig. 5. Dependence of the lattice parameters *a* and *c* and the CSR on the RTS temperature for the samples of isotropic hexaferrite $BaFe_{12}O_{19}$ (batch BH-12I).

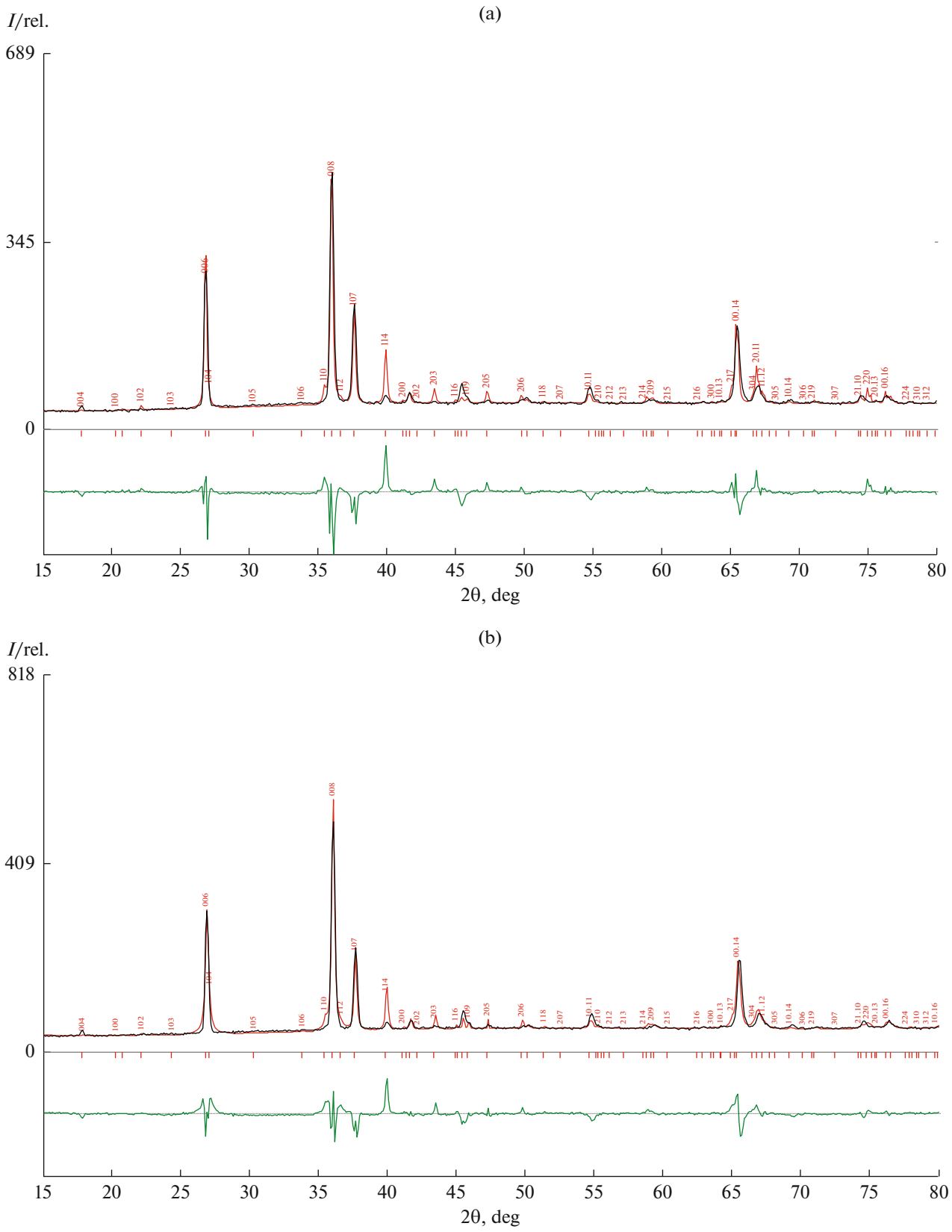

Fig. 6. Typical X-ray diffraction pattern of anisotropic hexaferrite $BaFe_{12}O_{19}$ (batch BH-12A) obtained by RTS at (a) 1200 and (b) 1250°C. 2θ values cover the range from 15° to 80°. Black line shows experimental data; red line, model; green line, difference spectrum.

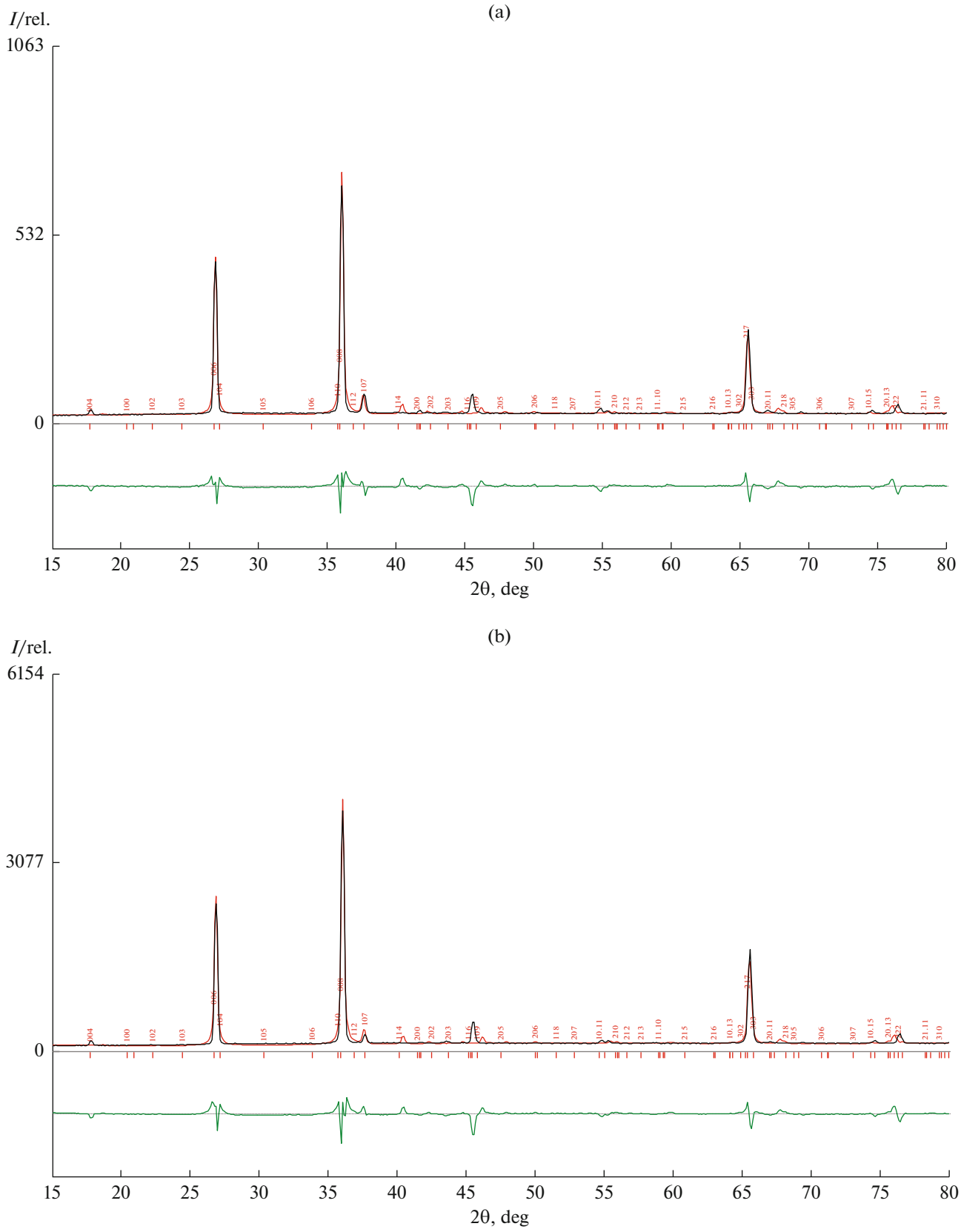

Fig. 7. Typical X-ray diffraction pattern of anisotropic hexaferrite $BaFe_{12}O_{19}$ (batch BH-12A) obtained by RTS at (a) 1300 and (b) 1350°C. 2θ values cover the range from 15° to 80°. Black line shows experimental data; red line, model; green line, difference spectrum.

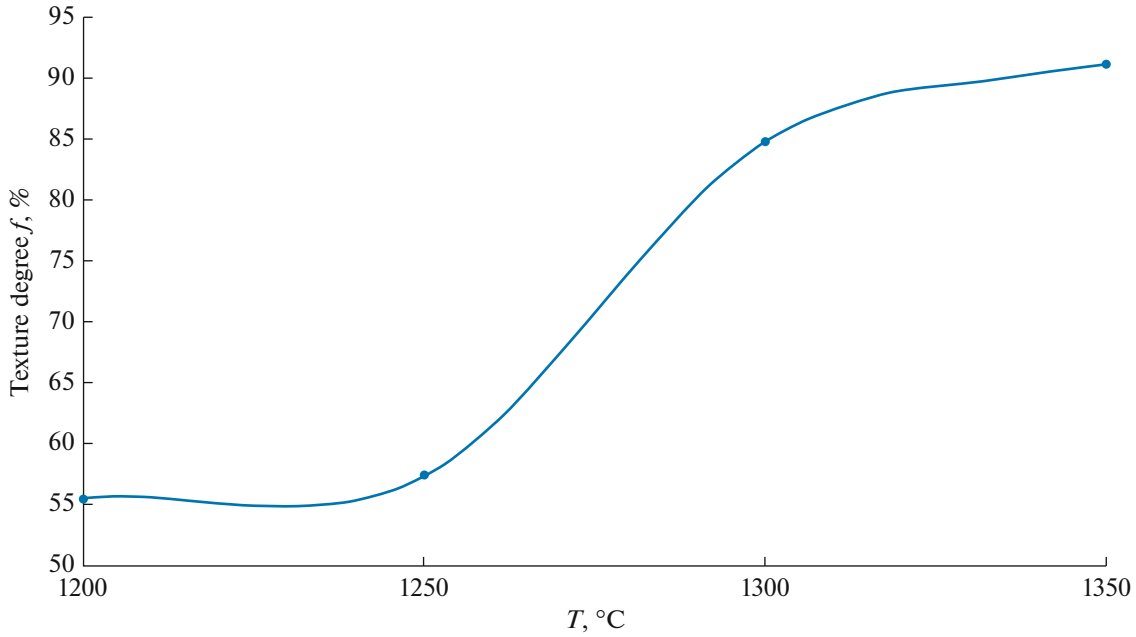

Fig. 8. Dependence of the degree of magnetic texture on the RTS temperature for the samples of anisotropic hexaferrite $BaFe_{12}O_{19}$ (batch BH-12A).

$BaFe_{12}O_{19}$ (ICSD #16157) [47]. All samples are characterized by a prominent plate-type texture with the shear plane (001). A phenomenon resembling phase transition is observed in the samples from this batch as the RTS temperature grows from 1200–1250 to 1300–1350°C: a sharp decrease in the parameter pref.orient.o1 from 0.38–0.40 to 0.26–0.28, simultaneous elongation of the crystal lattice along the [001] direction, and decrease in the hexagon edge.

Note that the Lorentzian curves were used to interpret the X-ray diffraction patterns of the samples grown at the sintering temperature of 1200 and 1250°C but the pseudo-Voigt shape of the line (a convolution of the Lorentzian and Gaussian shapes) should be taken instead to correctly describe the high-intensity reflexes of the (001) family. In addition, an unidentified peak between 45 and 46 degrees was found for the samples of the BH-12A batch obtained at 1300 and 1350°C. Different variants of interpreting this peak allowed us to conclude that it does not point to another phase but is a reflex belonging to the distorted hexaferrite structure.

According to the X-ray diffraction and calculations using Eq. (6), the degree of the magnetic texture f of the anisotropic hexaferrites (batch BH-12A) prepared by RTS at $T = 1200$°C is about 55%, and it grows further as the sintering temperature increases, achieving 91.3% at $T = 1350$°C (Fig. 8). It is worth noting that f usually increases as the sintering temperature increases also in the case of the classical thermal sintering of anisotropic hexaferrites. This is explained by the intensification of the recrystallization processes as the sintering temperature grows: small and "poorly" oriented crystallites are absorbed by larger crystals with a better orientation.

Figure 9 shows the dependences of the lattice parameters (a and c) and CSR in anisotropic hexaferrites $BaFe_{12}O_{19}$ (batch BH-12A) on the temperature of the RTS process. Evidently, parameter a remains the same at $T = 1250$ and 1200°C, decreases at $T > 1250$°C, and does not alter at 1300 and 1350°C. The lattice parameter c grows remarkably with the RTS temperature and achieves the value of $c = 23.2540$ at $T = 1300$°C. Further growth of T to 1350°C increases it only to $c = 23.2558$ nm.

The changes observed in the lattice parameters a and c of anisotropic hexaferrites from the BH-12A batch occurring at the increased RTS temperature indicate that the crystal lattice elongates along the direction [001] and the hexagon edge decreases.

No changes in the CSR of anisotropic hexaferrites from the BH-12A batch upon increasing the RTS temperature were observed.

The results presented above and findings of [46] count in favor of a strong correlation between the value of the crystalline texture parameter pref.orient.o1 and the degree of the magnetic texture. Allowing for the fact that the hexaferrites studied in this work (both isotropic and anisotropic) show a wide range of the degree of the magnetic texture, our aim was to find the mathematical dependence of the crystalline texture parameter pref.orient.o1 on the magnetic texture of parameter f for polycrystalline hexagonal barium ferrites.

Analysis of the values of pref.orient.o1 found in all the studied samples and comparing them with the cor-

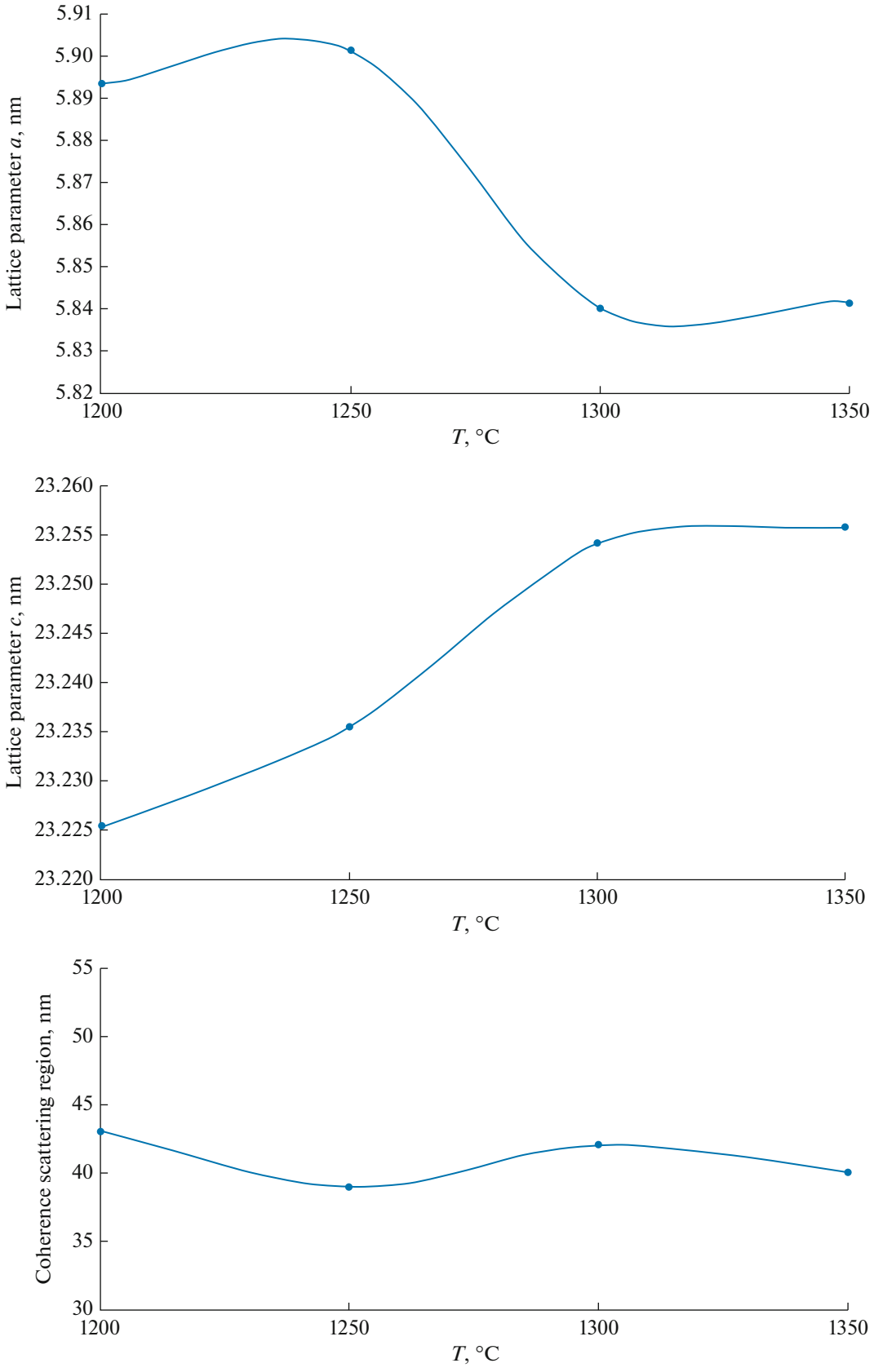

Fig. 9. Dependence of the lattice parameters *a* and *c* and the CSR on the RTS temperature for the samples of anisotropic hexaferrite $BaFe_{12}O_{19}$ (batch BH-12A).

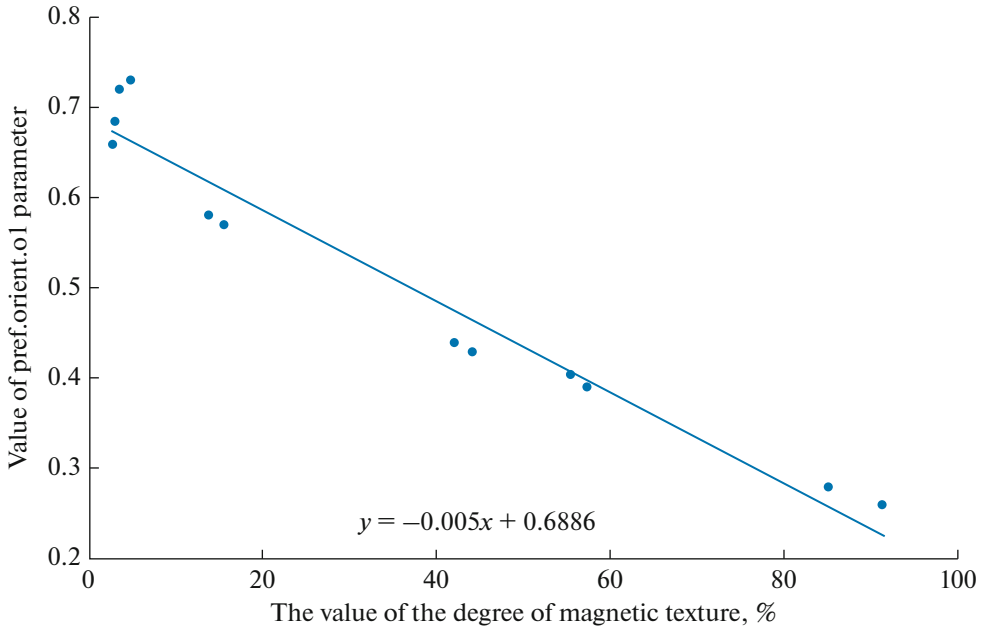

Fig. 10. Dependence of the parameter of the predominant orientation of the crystalline texture pref.orient.o1 on the degree of magnetic texture *f* in polycrystalline hexagonal barium ferrites.

responding degrees of the magnetic texture allowed us to conclude that there is a linear dependence between them (Fig. 10).

The mathematical expression for the straight line describing the found dependence is

$$\text{pref.orient.o1} = -0.005f + 0.6886, \quad (2)$$

where *f* is the degree of the texture (%).

3. CONCLUSIONS

It was shown for the first time that the RTS technology allows obtaining high-quality isotropic and anisotropic hexaferrites $BaFe_{12}O_{19}$ from crude blanks made of a ferritized charge. The features of the crystal structure and texture of the isotropic and anisotropic polycrystalline hexagonal barium ferrites $BaFe_{12}O_{19}$ obtained by the RTS method at the temperatures of 1200, 1250, 1300, and 1350°C were investigated by X-ray diffraction spectroscopy and X-ray phase analysis. The results obtained allow us to make the following conclusions.

(1) The only phase found in all the obtained and studied samples of polycrystalline hexagonal ferrites is hexaferrite. All the samples are monophasic and are characterized by the crystal structure of barium hexaferrite $BaFe_{12}O_{19}$ (ICSD #1657).

(2) A relatively prominent crystalline texture consisting of plates with the value of pref.orien.o1 ranging from 0.66 to 0.74 is typical of isotropic hexaferrite $BaFe_{12}O_{19}$; as the temperature of the RTS grows, the shear plane of the plates changes from (107) (at the sintering temperature of 1200 and 1250°C) to (001) (at 1300 and 1350°C).

(3) Despite the absence of a magnetic field during the compaction process, all the samples of isotropic hexaferrite $BaFe_{12}O_{19}$ possessed a small magnetic texture ranging from 3.0 to 4.9%. This texture arises due to the lamellar shape of the hexaferrite particles formed in the ferritizing process.

(4) An effect similar to a phase transition was observed upon increasing the RTS temperature from 1200–1250 to 1300–1350°C in anisotropic hexaferrites $BaFe_{12}O_{19}$: the parameter pref.orient.o1 decreases sharply from 0.38–0.40 to 0.26–0.28, the crystal lattice extends along the direction [001], and the hexagon edge is shortened. This effect should be related to the intensive formation of the magnetic texture at the temperatures of 1300 and 1350°C.

(5) The peak, which remained unidentified, between 45 and 46 degrees was found for anisotropic hexaferrite $BaFe_{12}O_{19}$ obtained by RTS at 1300 and 1350°C. This peak is one of the reflexes of the distorted hexaferrite structure.

(6) It was found for the first time that the dependence of the predominant orientation of the crystalline texture pref.orient.o1 on the degree of the magnetic texture *f* in M-type polycrystalline barium hexagonal ferrites is described by the expression pref.orient.o1 = –0.005*f* + 0.6886.

FUNDING

The work was partially supported by the Ministry of Science and Education of the Russian Federation under the

agreement on subsidy no. 14.575.21.0030 dated June 27, 2014 (RFMEFI57514X0030).

REFERENCES

1. Adelsköld, V., X-ray studies on magneto-plumbite, $PbO \cdot 6Fe_2O_3$ and other substances resembling 'beta-alumina', $Na_2O \cdot 11Al_2O_3$, *Ark. Kemi. Mineral. Geol.,* 1938, vol. 12A, no. 29, p. 1–9.
2. Ozgur, U., Alivov, Y., and Morkoc, H., Microwave ferrites, part 1: fundamental properties, *J. Mater. Sci.: Mater. Electron.,* 2009, vol. 20, no. 9, pp. 789–834.
3. Harris V.G, Modern microwave ferrites, *IEEE Trans. Mag.,* 2012, vol. 48, pp. 1075–1104.
4. *Microwave Ferrites and Ferrimagnetics,* Lax, B. and Button, K.J., Eds., New York: McGraw-Hill, 1962.
5. Shcherbakov, S.V., The development of microwave electronics in the framework of state programs, in *Materialy VI Vserossiiskoi nauchno-tekhnicheskoi konferentsii "Elektronika i mikroelektronika SVCh"* (Proceedings of the All-Russian Conference on Microwave Electronics and Microelectronics, St. Petersburg, May 29–June 1, 2017), pp. 15–23.
6. Shcherbakov, S.V., The development of microwave electronics in Russia, in *Materialy nauchno-tekhnicheskoi konferentsii "SVCh-elektronika-2016"* (Proceedings of the Conference on Microwave Electronics, Fryazino, May 18–19, 2016).
7. Ustinov, A., Kochemasov, V., and Khas'yanova, E., Ferrite materials for microwave electronics devices. Key selection criteria, *Elektron.: Nauka Tekhnol. Biznes,* 2015, no. 8 (00148), pp. 86–92.
8. Kharinskaya, M., Microwave ferrite materials. Well, how to do without microwave devices!, *Elektron.: Nauka Tekhnol. Biznes,* 2000, no. 1 (00148), pp. 24–27.
9. Letyuk, L.M., Kostishin, V.G., and Gonchar, A.V., *Tekhnologiya ferritovykh materialov magnitoelektroniki* (Technology of Ferrite Materials of Magnetoelectronics), Moscow: MISiS, 2005.
10. Antsiferov, V.N., Letyuk, L.M., Andreev, V.G., Kostishin, V.G., et al., *Problemy poroshkovogo materialovedeniya. Chast' V. Tekhnologiya proizvodstva poroshkovykh ferritovykh materialov. Uchebnik dlya studentov VUZov* (Problems of Powder Materials Science. Part V. Technology for the Production of Powder Ferrite Materials. The School-Book for Higher School), Ekaterinburg: UrO RAN, 2005.
11. Yakovlev, Yu.M. and Gendelev, S.Sh., *Monokristally ferritov v radioelektronike* (Single Ferrite Crystals in Electronics), Moscow: Sov. Radio, 1975.
12. Kostishyn, V.G., Korovushkin, V.V., Chitanov, D.N., and Korolev, Yu.M., Obtaining and properties of hexaferrite $BaFe_{12}O_{19}$ for high-coercivity permanent magnets and substrates microstrip microwave devices of mm-range, *J. Nano- Electron. Phys.,* 2015, vol. 7, no. 4, pp. 04057-1–04057-47. http://nbuv.gov.ua/UJRN/jnef_2015_7_4_59.
13. Andreev, V.G., Kostishyn, V.G., Ursulyak, N.D., Nalogin, A.G., and Kudashov, A.A., Influence of modes shredding of source components by processes to synthesis and activity of powder sintering hexaferrite, *J. Nano- Electron. Phys.,* 2015, vol. 7, no. 4, p. 04070. https://jnep.sumdu.edu.ua/download/numbers/2015/4/articles/jnep_2015_V7_04070.pdf.
14. Kostishyn, V.G., Panina, L.V., Timofeev, A.V., Kozhitov, L.V., Kovalev, A.N., and Zyuzin, A.K., Dual ferroic properties of hexagonal ferrite ceramics $BaFe_{12}O_{19}$ and $SrFe_{12}O_{19}$, 2016, vol. 400, pp. 327–332. https://doi.org/10.1016/j.jmmm.2015.09.011
15. Kostishyn, V.G., Panina, L.V., Kozhitov, L.V., Timofeev, A.V., and Kovalev, A.N., Synthesis and multiferroic properties of M-type $SrFe_{12}O_{19}$ hexaferrite ceramics, *J. Alloys Compd.,* 2015, vol. 645, pp. 297–300. https://doi.org/10.1016/j.jallcom.2015.05.024
16. Trukhanov, A.V., Trukhanov, S.V., Kostishyn, V.G., Panina, L.V., Korovushkin, V.V., Turchenko V. A, Vinnik, D.A., Yakovenko, E.S., Zagorodnii, V.V., Launetz, V.L., Oliynyk, V.V., Zubar, T.I., Tishkevich, D.I., and Trukhanova, E.L., Correlation of the atomic structure, magnetic properties and microwave characteristics in substituted hexagonal ferrites, *J. Magn. Magn. Mater.,* 2018, vol. 462, pp. 127–135. https://doi.org/10.1016/j.jmmm.2018.05.006
17. Trukhanov, A.V., Kostishyn, V.G., Panina, L.V., Korovushkin, V.V., Turchenko, V.A., Thakur, P., Thakur, A., Yang, Y., Vinnik, D.A., Yakovenko, E.S., Matzui, L.Yu., Trukhanova, E.L., and Trukhanov, S.V., Control of electromagnetic properties in substituted M-type hexagonal ferrites, *J. Alloys Compd.,* 2018, vol. 754, pp. 247–256. https://doi.org/10.1016/j.jallcom.2018.04.150
18. Gal'tseva, O.V., Solid-phase synthesis of lithium ferrites in an accelerated electron beam, *Cand. Sci. Dissertation,* Tomsk, 2009.
19. Vasendina, E.A., Radiation-thermal synthesis of doped lithium ferrites in an accelerated electron beam, *Cand. Sci. Dissertation,* Tomsk, 2011.
20. Gyngazov, S.A., Radiation-thermal activation of diffusion mass transfer in oxide ceramics, *Doctoral Dissertation,* Tomsk, 2011.
21. Lysenko, E.N., Radiation-thermal activation of oxygen diffusion in polycrystalline lithium-titanium ferrites, *Cand. Sci. Dissertation,* Tomsk, 2003.
22. Lysenko, E.N., Vasendina, E.A., Vlasov, V.A., Sokolovskii, A.N., Kondratyuk, A.A., and Gal'tseva, O.V., Magnetization of a Li_2CO_3–Fe_2O_3–ZnO powdered mixture ferritized in an accelerated electron beam, *Izv. Vyssh. Uchebn. Zaved., Fiz.,* 2000, no. 1/3, pp. 71–74.
23. Usmanov, R.U., The formation of the structure and magnetic properties of polycrystalline lithium-titanium ferrites during radiation-thermal exposure, *Cand. Sci. Dissertation,* Tomsk, 2005.
24. Shabardin, R.S., Development of technology for radiation-thermal sintering of lithium-titanium ferrite ceramics, *Cand. Sci. Dissertation,* Tomsk, 2004.
25. Surzhikov, A.R., Pritulov, A.M., Lysenko, E.N., Sokolovskiy, A.N., Vlasov, V.A., and Vasendina, E.A., Calorimetric investigation of radiation-thermal synthesized lithium pentaferrite, *J. Therm. Anal. Calorim.,* 2010, vol. 101, pp. 11–13.
26. Surzhikov, A.R., Pritulov, A.M., Usmanov, R.U., and Galtseva, O.V., Synthesis of lithium orthoferrite in the beam of accelerated electrons, in *Chaos and Structures in Nonliniear Systems. Theory and Experiment,* Astana: ENU, 2006, pp. 198–200.

27. Surzhikov, A.P., Pritulov, A.M., Gal'tseva, O.B., Usmanov, R.U., Malyshev, A.V., and Bezuglov, V.V., The influence of the degree of compaction of reagents on the solid-phase synthesis of lithium pentaferrite in an accelerated electron beam, in *Radiatsionnaya fizika tverdogo tela* (Radiation Solid State Physics), Moscow: GNU NII MPT, 2007, pp. 475–478.

28. Surzhikov, A.P., Pritulov, A.M., Gal'tseva, O.V., Usmanov, R.U., Sokolovskii, A.N., and Vlasov, B.A., Formal kinetic analysis of solid-phase synthesis of lithium pentaferrite in an accelerated electron beam, in *Radiatsionnaya fizika tverdogo tela* (Radiation Solid State Physics), Moscow: NII MIT, 2008, pp. 365–371.

29. Surzhikov, A.P., Radiation-thermal sintering of ferrite ceramics, *Extended Abstract of Doctoral (Phys. Math.) Dissertation,* Blagoveshchensk, 1993.

30. Kostishin, V.G., Andreev, V.G., Kaneva, I.I., Panina, L.V., Chitanov, D.N., Yudanov, N.A., Komlev, A.S., and Nikolaev, A.N., Obtaining by method of radiation-thermal sintering MgZn-ferrites with a level of properties of NiZn-ferrite grade 600NN, *Izv. Yugo-Zap. Univ.,* 2013, no. 5 (50), pp. 228–235.

31. Kostishin, V.G., Korovushkin, V.V., Panina, L.V., Komlev, A.V., Yudanov, N.A., Adamtsov, A.Yu., Nikolaev, A.N., and Andreev, V.G., Structure and properties of MnZn-ferrite ceramics obtained by radiation thermal sintering, *Izv. Yugo-Zap. Univ., Ser.: Tekh. Tekhnol.,* 2013, no. 2, pp. 053–059.

32. Kostishin, V.G., Kozhitov, L.V., Korovushkin, V.V., Andreev, V.G., Chitanov, D.N., Yudanov, N.A., Morchenko, A.T., Komlev, A.S., Adamtsov, A.Yu., and Nikolaev, A.N., Production of 2000NN soft magnetic ferrites by radiation thermal sintering from a pre-ferritized charge and from a charge without ferritization, *Izv. Yugo-Zap. Univ., Ser.: Fiz. Khim.,* 2013, no. 2, pp. 008–018.

33. Kostishin, V.G., Andreev, V.G., Korovushkin, V.V., Chitanov, D.N., Yudanov, N.A., Morchenko, A.T., Komlev, A.S., Adamtsov, A.Yu., and Nikolaev, A.N., Preparation of 2000NN ferrite ceramics by a complete and a short radiation-enhanced thermal sintering process, *Inorg. Mater.,* 2014, vol. 50, no. 12, pp. 1317–1324.

34. Kostishin, V.G., Andreev, V.G., Panina, L.V., Chitanov, D.N., Yudanov, N.A., Komlev, A.S., and Nikolaev, A.N., Soft-magnetic Mg–Zn ferrite ceramics comparable in performance to 600NN Ni–Zn ferrite: fabrication by radiation-enhanced thermal sintering, *Inorg. Mater.,* 2014, vol. 50, no. 11, pp. 1174–1178.

35. Kostishin, V.G., Korovushkin, V.V., Panina, L.V., Andreev, V.G., Komlev, A.S., Yudanov, N.A., Adamtsov, A.Yu., and Nikolaev, A.N., Magnetic structure and properties of Mn–Zn ferrites prepared by radiation-enhanced thermal sintering, *Inorg. Mater.,* 2014, vol. 50, no. 12, pp. 1252–1256.

36. Kiselev, B.G., Kostishin, V.G., Komlev, A.S., and Lomonosova, N.V., Substantiation of economic advantages of technology of radiation-thermal agglomeration of ferrite ceramics, *Tsvetn. Met.,* 2015, vol. 2015, no. 4, pp. 7–11.

37. Kostishyn, V.G., Komlev, A.S., Korobeynikov, M.V., Bryazgin, A.A., Shvedunov, V.I., Timofeev, A.V., and Mikhailenko, M.A., Effect of a temperature mode of radiation-thermal sintering the structure and magnetic properties of Mn–Zn-ferrites, *J. Nano- Electron. Phys.,* 2015, vol. 7, no. 4, p. 04044.

38. Kostishyn, V., Isaev, I., Scherbakov, S., Nalogin, A., Belokon, E., and Bryazgin, A., Obtaining anisotropic hexaferrites for the base layers of microstrip SHF devices by the radiation-thermal sintering, *East.-Eur. J. Enterprise Technol.,* 2016, no. 5/8 (83), pp. 32–39.

39. Kostishin V.G. Isaev, I.M., Chitanov, D.N., Komlev, A.S., Shcherbakov, S.V., et al., Obtaining by radiation-thermal sintering of anisotropic hexagonal ferrites for substrates of microstrip microwave devices of mm-wavelength range, in *Materialy XXIV Mezhdunarodnoi konferentsii "Elektromagnitnoe pole i materialy (fundamental'nye fizicheskie isledovaniya)"* (Proceedings of the 24th International Conference on Electromagnetic Field and Materials (Fundamental Physical Research)), Moscow, Nov. 18–19, 2016), pp. 396–407.

40. Komlev, A.S., Radiation-thermal sintering in a beam of fast electrons of polycrystalline ferrospinels, *Extended Abstract of Cand. Sci. (Tech. Sci.) Dissertation,* Moscow, 2018.

41. Kostishin, V.G., Isaev, I.M., Komlev, A.S., Timofeev, A.V., Shcherbakov, S.V., et al., Features of the crystal structure and phase composition of anisotropic hexagonal ferrites $BaFe_{12}O_{19}$ and $BaFe_{9.5}Al_{2.5}O_{19}$ obtained by radiation thermal sintering, in *Materialy XXIV Mezhdunarodnoi konferentsii "Elektromagnitnoe pole i materialy (fundamental'nye fizicheskie isledovaniya)"* (Proceedings of the 24th International Conference on Electromagnetic Field and Materials (Fundamental Physical Research)), Moscow, Nov. 18–19, 2016), pp. 409–424.

42. Naiden, E.P., Minin, R.V., Itin, V.I., and Zhuravlev, V.A., Influence of radiation-thermal treatment on the phase composition and structural parameters of the SHS product based on W-type hexaferrite, *Russ. Phys. J.,* 2013, vol. 56, no. 6, pp. 674–680.

43. Zhuravlev, V.A., Naiden, E.P., Minin, R.V., et al., Radiation-thermal synthesis of W-hexaferrites, in *Proceedings of the International Scientific Conference on Radiation-Thermal Effects and Processes in Inorganic Materials 2015 (RTEP2015), IOP Conf. Ser.: Mater. Sci. Eng.,* 2015, vol. 81, p. 012003. https://doi.org/10.1088/1757-899X/81/1/012003

44. Naiden, E.P., Zhuravlev, V.A., Minin, R.V., et al., Structural and magnetic properties of SHS-produced multiphase W-type hexaferrites: influence of radiation thermal treatment, *Int. J. Self-Propag. High-Temp. Synth.,* 2015, vol. 24, no. 3, pp. 148–151.

45. Komlev, A.S., Isaev, I.M., Kostishin, V.G., Chitanov, D.N., and Timofeev, A.V., Cell for radiation thermal sintering, Available from MISiS no. 81-219-2016, 2016.

46. Toraya H. and Marumo, F., Preferred orientation correction in powder patter-fitting, *Mineral. J.,* 1981, vol. 10, no. 5, pp. 211–221.

47. Database for Fully Identified Inorganic Crystalline Structures. https://icsd.fiz-karlsruhe.de/search/.

48. Kaneva, I.I., Kostishin, V.G., Andreev, V.G., et al., Obtaining barium hexaferrite with enhanced isotropic properties, *Izv. Vyssh. Uchebn. Zaved., Mater. Elektron. Tekh.,* 2014, vol. 17, no. 3, pp. 183–188.

Translated by S. Efimov